Journal of
Materials Chemistry A

Accepted Manuscript

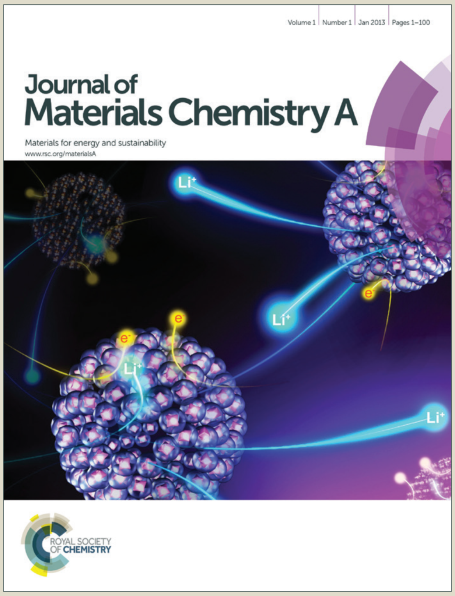

ROYAL SOCIETY
OF **CHEMISTRY**

www.rsc.org/materialsA

Journal Name

Journal of Materials Chemistry A

Dynamic Article Links ►

Cite this: DOI: 10.1039/c0xx00000x

www.rsc.org/xxxxxx

ARTICLE TYPE

Self-Assembled Ultrathin Titania Nanosheets as Blocking Layers for Significantly Enhanced Photocurrent and Photovoltage of Dye-Sensitized Solar Cells

Lu Zhang,[1] Hong Sun,[1] Zhaosheng Xue,[2] Bin Liu,[2,3] Zhong-Sheng Wang[1,*]

Received (in XXX, XXX) Xth XXXXXXXXX 20XX, Accepted Xth XXXXXXXXX 20XX
DOI: 10.1039/b000000x

To retard charge recombination efficiently in dye-sensitized solar cells (DSSCs), an ultrathin film of single-crystal titania nanosheets is pre-coated on the conductive substrate as a blocking layer through electrostatic layer-by-layer self-assembly. The marked effect of self-assembled titania nanosheet film is the remarkable enhancements of short-circuit photocurrent by 45%, from 12.57 to 18.24 mA cm^{-2}, and open-circuit photovoltage by 16%, from 690 to 798 mV. As a consequence, power conversion efficiency is improved notably by 61% from 6.50% to 10.48% when 50 nm thick titania nanosheets film is pre-coated as a blocking layer, which is also superior to the pyrolyzed blocking layer (7.79%) and the well-known $TiCl_4$ treatment (efficiency of 7.98%). Controlled intensity modulated photovoltage/photocurrent spectra reveal that the self-assembled blocking layer of titania nanosheets not only retards charge recombination but also increases charge collection efficiency, accounting for the remarkable increase in open-circuit photovoltage and short-circuit photocurrent, respectively. This finding implies that pre-deposition of ultrathin TiO_2 nanosheet layer on the conductive substrate would be an ideal strategy to remarkably increase short-circuit photocurrent and open-circuit photovoltage simultaneously and thus to enhance power conversion efficiency of DSSCs remarkably.

Introduction

Since the milestone discovery by O'Regan and Grätzel,[1] interests in dye-sensitized solar cells (DSSCs) have grown continuously as they are potential cost-effective alternatives to the conventional silicon-based p-n junction solar cells. A typical DSSC device comprises a dye-sensitized nanocrystalline porous TiO_2 film deposited on the conductive substrate (e.g. fluorine doped tin oxide, FTO) as the working electrode, a Pt-coated FTO as the counter electrode, and a redox-couple-contained (e.g. I_3^-/I^-) solution as the electrolyte filling the space between the working and counter electrodes and penetrating throughout the porous TiO_2 film. To improve solar cell performance, great efforts have been made by developing efficient dye sensitizers,[2,3] redox couples,[4] and electrocatalysts.[5,6]

Besides the optimization of photoanode structures[7,8] in DSSCs, suppression of charge recombination is also necessary to achieve high efficiency. Charge recombination takes place at the FTO/electrolyte and TiO_2/electrolyte interfaces, which is the main mechanism for performance losses.[9,10] To obtain high efficiency, a barrier layer is needed to deposit onto the FTO surface.[10-13]

Electron recombination losses are remarkable at the FTO/electrolyte interface particularly at the point of maximum power or at open circuit.[9-11] To minimize the electron losses arising from the charge recombination at the FTO/electrolyte interface, a dense TiO_2 nanoparticle blocking layer is deposited onto FTO using various techniques, such as magnetron sputtering,[11,14] atomic layer deposition (ALD),[15] electrochemical deposition,[15] sol-gel processing[16] and spray pyrolysis.[9,13,15] Improvements of efficiency have been achieved by using these blocking layers. Kavan et al. electrochemically evaluated the quality of ALD, electrodeposited, and spray pyrolyzed TiO_2 blocking layers by quantifying the effective area of pinholes in the blocking layer using redox probes.[15] They point out that spray pyrolysis is the method of choice taking the blocking effect and coating procedures into account.[15] However, it is very difficult for pyrolyzed TiO_2 nanoparticles to fully cover the FTO surface. The effective pinhole area relative to the projected electrode area is reported to be >40% for the pyrolyzed blocking layer.[15] For this reason, the efficiency enhancement resulting from the pyrolyzed blocking layer is not very notable. Therefore, it is still challenging to develop a more compact blocking layer for fabrication of high-performance DSSCs.

In this study we report self-assembled single-crystal titania nanosheet film on the conductive glass as the blocking layer in DSSCs to suppress charge recombination. The flat nanosheets are possible to fully cover the surface of FTO, which is important to protect the collected electrons at the FTO from recombination with the electrolyte. Moreover, it is expected for flat nanosheets to have more and better contacts with FTO, which, in combination with the single-crystal feature of nanosheet, enables efficient electron transport from the nanocrystalline TiO_2 film to the underlying TiO_2 nanosheet blocking layer and then to the conductive substrate for efficient electron collection. Finally, the simple and cost-effective self-assembly technique is conductive to control the thickness of the blocking layer precisely, which is critical to optimize the blocking effect. The experimental results reveal that the pre-coating of ~50 nm titania nanosheet layer on FTO increases short-circuit photocurrent, open-circuit photovoltage and power conversion efficiency remarkably, which also outperforms the pyrolyzed TiO_2 nanoparticle blocking layer and the typical $TiCl_4$ treatment.

Experimental

Materials. Poly(diallyldimethylammonium chloride) (PDDA, molecular weight $1\times10^5 - 2\times10^5$), I_2, LiI, 4-tert-butylpyridine (TBP) were obtained from Acros. 1, 2-dimethyl-3-n-propylimidazolium iodide (DMPII) was available from our previous study.[17] H_2PtCl_6 was purchased from Sinopharm Chemical Reagent Co., China. Conductive glass (fluorine-doped SnO_2, FTO, 14 Ω/square, transmittance 85%) was purchased from Nippon Sheet Glass Co., Japan. Cis-di(isothiocyanato)-bis-(2,2′-bipyridyl-4,4′-dicarboxylato) ruthenium(II) bis-tetrabutylammonium (the so-called N719) was purchased from Lumtec Corp., Taiwan, P. R. China.

Synthesis of TiO_2 Nanosheets. Single-crystalline anatase titania nanosheets were synthesized from a hydrothermal method as described in a previous report[18] using hydrofluoric acid as a morphology controlling agent and titanium tetrabutoxide, $Ti(OC_4H_9)_4$, as the precursor. Briefly, 5 mL of $Ti(OC_4H_9)_4$ was mixed with 0.6 mL of hydrofluoric acid solution (47wt%), which was then transferred to a Teflon-lined autoclave followed by heating at 180 °C for 24 h. The yielded white powder was separated by high-speed centrifugation and washed with ethanol and distilled water for three times followed by drying in an oven at 80 °C for 6 h.

Self-Assembled Ultrathin Layer of TiO_2 Nanosheets on FTO. The titania nanosheets were dispersed in water (0.2 g dm^{-3}), which was adjusted to pH9 with tetrabutylammonium hydroxide in order to induce negative charges on the nanosheet's surface.[19] PDDA aqueous solution (20 g dm^{-3}, pH9) containing 0.5 M NaCl was used as the counterpart of negatively charged nanosheets due to the polycation characteristic. Ultrathin titania nanosheet layers were deposited on the FTO substrate with a typical electrostatic layer-by-layer self-assembly (ELSA) technique[20] by sequentially dipping the substrate in PDDA solution and titania nanosheet colloid for 20 min each. Multilayer films of $FTO/(PDDA/NS)_n$ were obtained by repeating the above ELSA cycle for *n* times, where NS represented titania nanosheets. The PDDA was burnt out by sintering the self-assembled film at 500 °C for 1 h, and the film was then converted to $FTO/(NS)_n$.

Fabrication of DSSCs. The nanocrystalline TiO_2 film (22 μm), composed of 25 nm TiO_2 nanoparticles,[21] was respectively screen printed onto uncoated FTO and titania nanosheets pre-coated FTO followed by sintering at 500 °C for 1 h. N719 was used as the dye sensitizer. The electrolyte was 0.6 M DMPImI, 0.1 M LiI, 0.05 M I_2, 0.5 M TBP dissolved in anhydrous acetonitrile. The counter electrode was fabricated by pyrolysis of H_2PtCl_6 solution in propanol on FTO. The DSSCs were assembled and sealed for this study; the fabrication methods were well documented in the literature.[6] The measurements of photovoltaic performance, controlled intensity modulated photovoltage/photocurrent spectra (IMVS/IMPS) for DSSCs, and the characterizations of materials are detailed in the Electronic Supplementary Information (ESI).

Results and discussion

Self-Assembly of Titania Nanosheets on FTO. The TiO_2 nanosheets are rectangular with side length of 20-50 nm and thickness of ~5 nm as confirmed by transmission electron microscopy (TEM, Figure S1) and field-emitting scanning electron microscopy (SEM, Figure S2). The sample shows anatase phase as revealed by the X-ray diffraction (XRD) patterns (Figure S3). The high-resolution TEM image (Figure S4a) reveals the clear lattice fringes, corresponding to the (001) planes of anatase TiO_2. Diffraction spots are observed in the selected-area electron diffraction (SAED) pattern (Figure S4b), confirming the single crystal feature of the obtained TiO_2 nanosheets. These characterization results are consistent with the previous report.[18] Since the TiO_2 nanosheets are negatively charged in a basic medium, we used PDDA, a polycation, for ELSA. Figure 1 shows the UV-vis absorption spectra for the self-assembled films on the quartz substrate after sintering at 500 °C, where the absorption peak at 270 nm is the characteristic of titania nanosheets.[22] The relationship between the absorbance at 270 nm and the number of bilayer is plotted in the inset of Figure 1. It is noted that the absorbance is the contribution of bilayer as the self-assembled film can grow on both sides of the quartz substrate. The growth of multilayers is confirmed by the progressive increment of absorption with layer number. The absorbance at 270 nm increases linearly with the number of bilayer (inset of Figure 1), indicating that each layer contains nearly equal amount of titania nanosheets. Contrasting to the spray pyrolysis and simple dip coating, which is difficult to control the layer thickness, the ELSA technique is able to tune the film thickness. The regular growth of nanosheet film via ELSA is advantageous to obtain a suitable thickness.

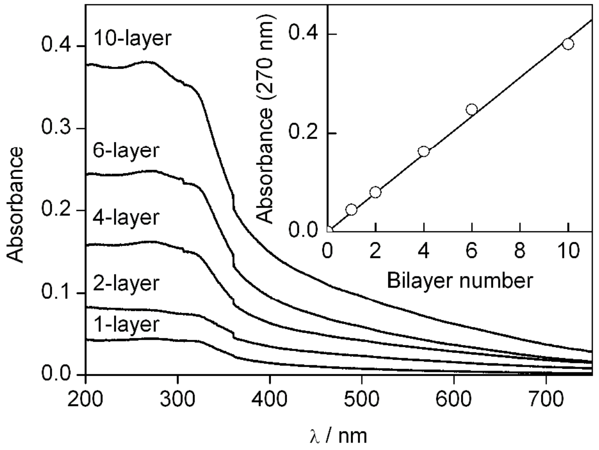

Figure 1. UV-vis absorption spectra for the self-assembled titania nanosheet films sintered at 500 °C for 1 h.

The surface morphology of the self-assembled film was examined with SEM. As compared to the bare FTO (Figure 2a), titania nanosheets can be seen in the monolayer film (Figure 2b), where titania nanosheets cover the FTO surface partially. The coverage of FTO with titania nanosheets increases with the number of self-assembled layer. For 10-layer nanosheets deposition, complete coverage is realized, as seen in Figure 2c. After calcination, the nanosheet hardly changes in size, and the nanosheet film has a relatively uniform size distribution in the range of 20-50 nm; the size of most nanosheets is 30-40 nm. A flat nanosheet layer on top of FTO can be observed from the cross-sectional SEM image (Figure 2d). For clear observation of the blocking layer, magnified cross-sectional SEM images is shown in Figure S5. The thickness of the 10-layer self-assembled film is determined to be 48-52 nm. The average thickness of each layer is calculated of 4.8-5.2 nm, which is in accordance with the thickness of titania nanosheet determined with TEM (Figure S1). The sheet resistance of FTO upon nanosheet deposition increases with increasing the blocking layer thickness, as listed in Table S1. The film resistance for ~50 nm nanosheet layer is 60 Ω/square, which is comparable to that (~55 Ω/square) for the dense TiO_2 nanoparticle layer formed by pyrolysis.

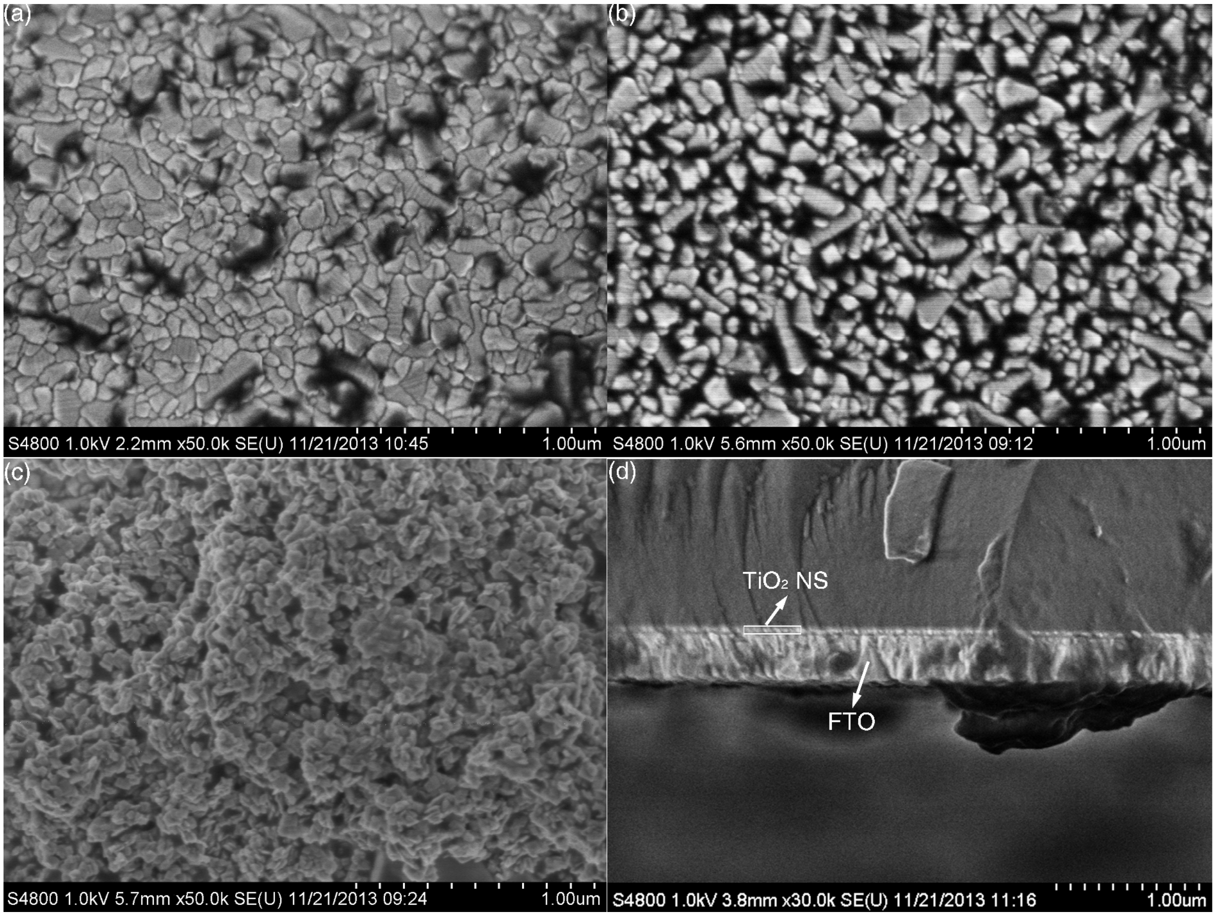

Figure 2. Top views of SEM images for the bare FTO (a), monolayer titania nanosheet film (b), and 10-layer titania nanosheet film (c); side view of SEM image for the 10-layer titania nanosheet film (d)

Photovoltaic Performance. To investigate the effect of pre-coated titania nanosheets and optimize solar cell performance, we pre-deposited titania nanosheet films on FTO with various thicknesses, which was controlled by the cycle number of self-assembly. The uncoated and pre-coated samples are denoted as $FTO/(NS)_n/TiO_2$, where n is the layer number of nanosheets and n = 0 represents the uncoated photoanode. Figure 3 presents the dependence of photovoltaic performance parameters on layer number. For the untreated DSSC (n = 0), the power conversion efficiency (*PCE*) was 6.55±0.10% with an average short-circuit photocurrent (J_{sc}) of 12.77 mA cm^{-2}, an open-circuit photovoltage (V_{oc}) of 693 mV and a fill factor (*FF*) of 0.74. Upon pre-coating of titania nanosheets, both J_{sc} and V_{oc} increased gradually up to 10 layers and then decreased gradually with further increasing the layer number. Although the film resistance increased with film thickness, the *FF* varied little with increasing the blocking layer thickness up to 100 nm and then dropped more significantly for thicker blocking layer, because there is an electron tunnelling effect for thinner blocking layer but the thicker layer may inhibit electron transport from photoanode to FTO. As a consequence, the *PCE* changed in the same trend of J_{sc}. Remarkably, monolayer nanosheet achieves *PCE* of >8%, which is 25% higher than that for the untreated sample. The highest *PCE* was achieved when 10 layers of titania nanosheets were pre-coated on FTO, and thus the 10-layer pre-coating was selected for further investigations on solar cell performance and the corresponding kinetics of charge transport and charge recombination.

Cite this: DOI: 10.1039/c0xx00000x

www.rsc.org/xxxxxx

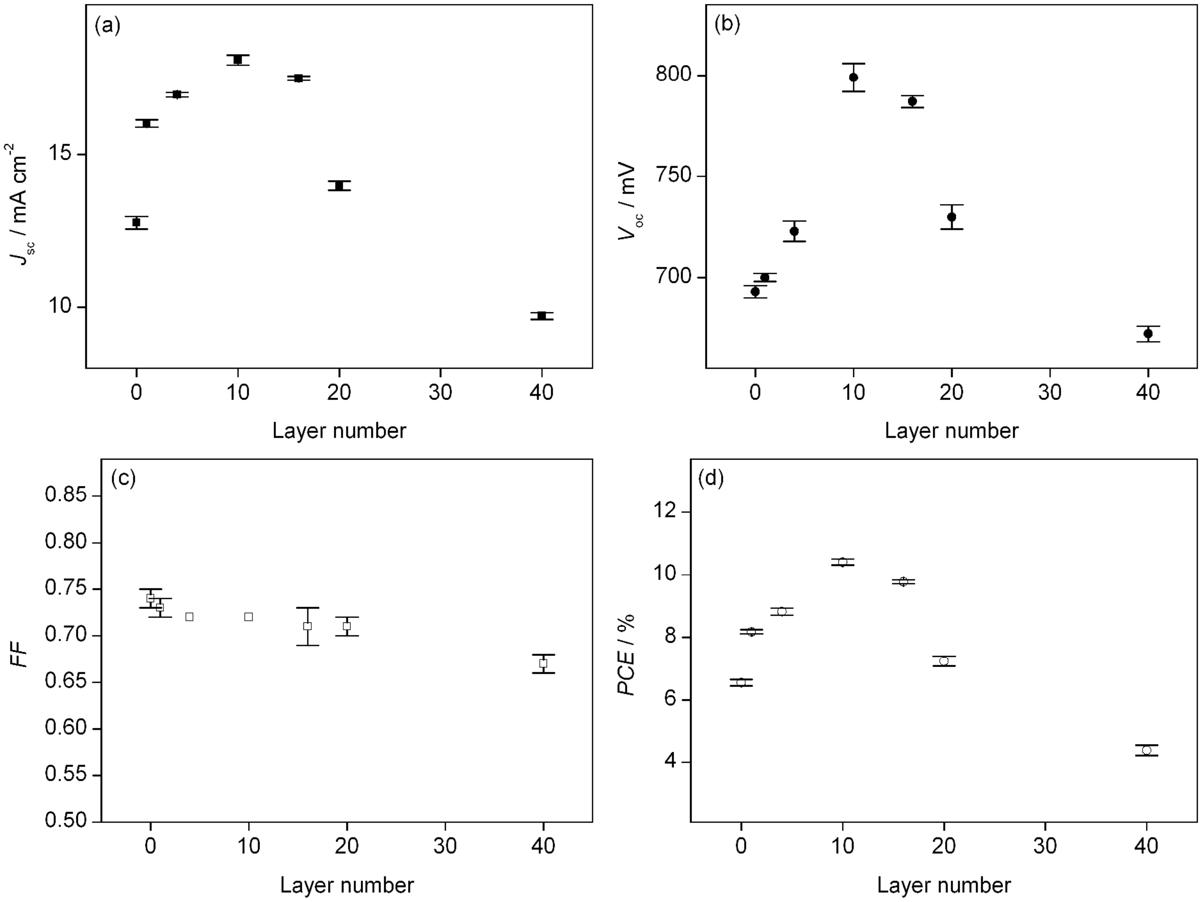

Figure 3. Dependence of J_{sc}, V_{oc}, *FF*, and *PCE* on layer number of titania nanosheets

Figure 4 shows the current-voltage characteristics of the fabricated DSSCs. For the untreated photoanode, the *PCE* was 6.50% with a J_{sc} of 12.57 mA cm^{-2}, a V_{oc} of 690 mV, and an *FF* of 0.75. Upon 10-layer nanosheets pre-coated on FTO, the *PCE* was improved notably to 10.48% with a J_{sc} of 18.24 mA cm^{-2}, a V_{oc} of 798 mV, and an *FF* of 0.72. As compared to the untreated photoanode, the J_{sc} was enhanced by 45% and the V_{oc} was lifted by 108 mV, resulting in improvement of *PCE* by 61%. As a control sample, the DSSC having the typical compact TiO_2 nanoparticle blocking layer (~50 nm) formed by pyrolysis gave *PCE* of 7.79% with a J_{sc} of 14.02 mA cm^{-2}, a V_{oc} of 751 mV, and an *FF* of 0.74. The TiO_2 nanoparticle blocking layer improved J_{sc}, V_{oc} and *PCE* relative to the untreated sample, but the improvements are less significant as compared to the nanosheet-blocking layer. As $TiCl_4$ treatment is the most often used treatment for high-performance DSSCs, it is interesting to demonstrate its performance. As seen in Figure 4, the $TiCl_4$ treatment yielded *PCE* of 7.98% with a J_{sc} of 16.13 mA cm^{-2}, a V_{oc} of 687 mV, and an *FF* of 0.72 (Figure 4). Consistent with the literature reports.[23,24] the $TiCl_4$ treatment improved the photocurrent significantly rather than the photovoltage, as compared to the untreated DSSC. By comparison, pre-coating of titania nanosheets (50 nm) is evidently superior to both the dense TiO_2 nanoparticle blocking layer and the well-known $TiCl_4$ treatment in terms of enhancements of photocurrent, photovoltage and efficiency.

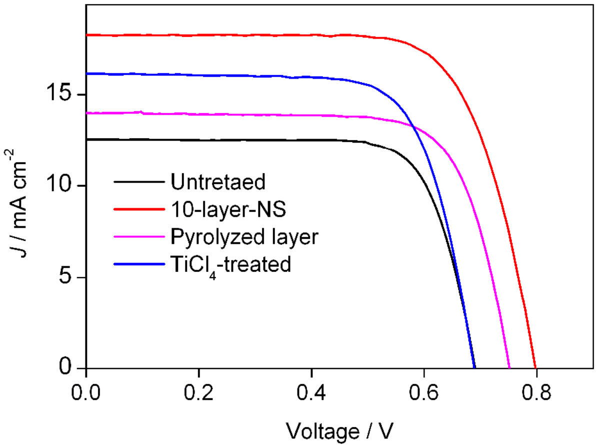

Figure 4. Current-voltage curves for the DSSCs with and without blocking layers under illumination of simulated AM1.5G solar light (100 mW cm^{-2})

As the only difference of the device structure for these DSSCs is the pre-coated titania nanosheet layer, the pre-coating of titania nanosheets on FTO should be responsible for the improved photocurrent and photovoltage. Next we will discuss the effect of pre-coated titania nanosheets on the position of conduction band (CB) edge of TiO_2, charge recombination and electron transport, which are the main factors influencing the photovoltaic performance.

Conduction Band Edge Level. For a DSSC with a given dye and electrolyte, the CB edge level of TiO_2 determines the driving force for electron injection and device photovoltage as well. It is thus important to determine the possible CB shift upon pre-coating of titania nanosheets. Figure 5 displays the dependence of V_{oc} on the photoinduced charge density (Q) at open circuit. For each photoanode, the V_{oc} increases linearly with the logarithm of Q, indicating that the photoinduced charge density increases exponentially with the V_{oc}.[25] The slopes, which are similar before and after pre-coating, are determined of 215 mV by linear fitting of V_{oc} and ln(Q). The V_{oc} of the untreated photoanode is the same as that for the titania nanosheets or nanoparticles pre-coated photoanode at the same charge density, indicating that the pre-coating does not alter the CB edge position.[25]

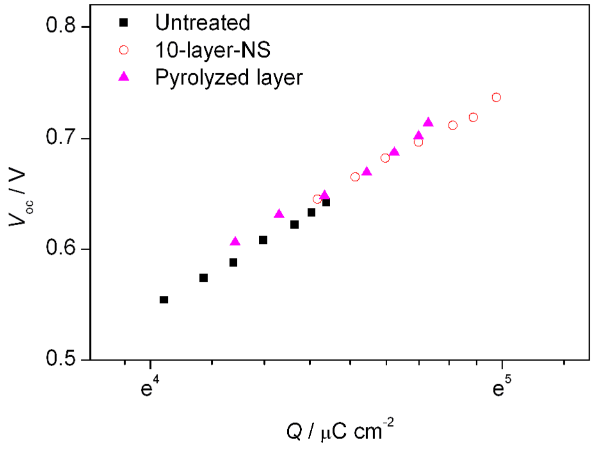

Figure 5. Dependence of V_{oc} on charge density at open circuit

Electron Transport. The electron transport time (τ_d) is obtained from the IMPS measurement at short circuit. The frequency (f_{min}) at minimum IMPS response determines the electron transport time following the expression $\tau_d = (2\pi f_{min})^{-1}$. Figure 6 presents log-log plot of τ_d with J_{sc}. The transport time decreases with J_{sc}, which is ascribed to the trapping/detrapping events. At the same photocurrent, the pre-coated nanosheet or nanoparticle layer does not affect the electron transport time obviously, implying that electron diffusion rate is not changed by the titania nanosheet or nanoparticle pre-coating. As the titania film does not change in the absence and presence of pre-coated ultra-thin titania nanosheets or nanoparticles, it is reasonable to observe comparable electron transport time constants.

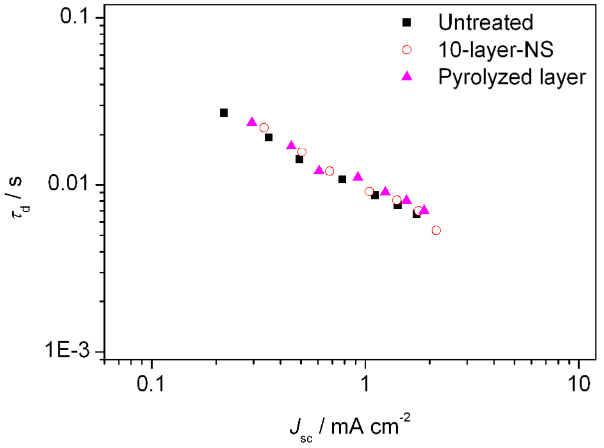

Figure 6. Electron transport time as a function of short-circuit photocurrent

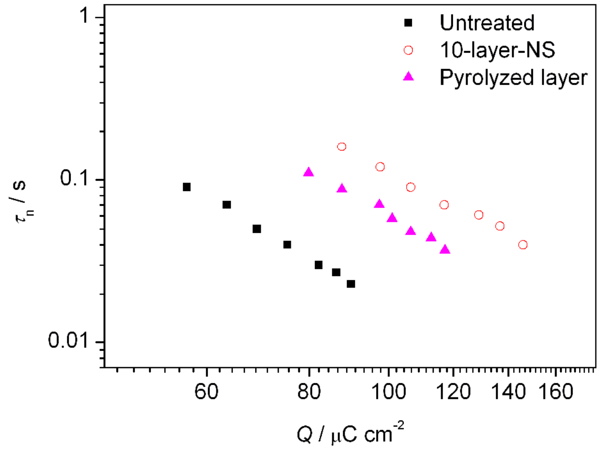

Figure 7. Electron lifetime as a function of charge density at open circuit

Charge Recombination. The electron lifetime (τ_n) is derived from the IMVS measurement according to the expression $\tau_r = (2\pi f_{min})^{-1}$, where f_{min} is the frequency at minimum IMVS response. Figure 7 shows the electron lifetimes as a function of charge density at open circuit in double logarithmic plot. The electron lifetime follows a power law function of charge density at open circuit with an exponent of 3.0. The pre-coated nanosheet or nanoparticle layer has a significant effect on the electron lifetime as observed in Figure 7. The electron lifetime at a given charge density is enhanced by 3.2-fold and 6.5-fold upon 50 nm titania nanoparticles and nanosheets pre-coated on the FTO surface, respectively. This indicates that covering FTO with 50 nm titania nanoparticle or nanosheet layer is effective to retard charge recombination between electrons and triiodides in the electrolyte. As compared to the pyrolyzed nanoparticle layer as a control sample, the nanosheet layer has a better blocking effect, as the electron lifetime at the same charge density for the latter is two times that for the former. The origin of such a good blocking effect will be studied in detail in the coming work.

Charge Collection and Electron Diffusion Length. Charge collection efficiency (η_{cc}) is an important factor in determining photocurrent generation for a given dye/electrolyte system, which is usually estimated by the electron transport time and electron lifetime following $\eta_{cc} = 1 - \tau_d/\tau_n$.[26] Figure 8a shows the charge collection efficiency as a function of light intensity. The η_{cc} is almost independent of light intensity for each photoanode, and it is enhanced from 71% to 87% upon pre-coating of titania nanosheets on FTO. Figure 8b presents the electron diffusion length (L_n) as a function of light intensity. The L_n is defined as $L_n = (d^2 \times \tau_n/4\tau_d)^{1/2}$, where d is the film thickness. For each photoanode, the L_n hardly changes with light intensity. Upon pre-coating of titania nanosheets, the L_n increases from 20 to 30 μm by 50%. As a control sample, the pyrolyzed nanoparticle layer gave η_{cc} of ~80% and L_n of ~25 μm (Figure 8). Evidently, the nanosheet blocking layer is superior to the pyrolyzed nanoparticle layer in charge collection efficiency.

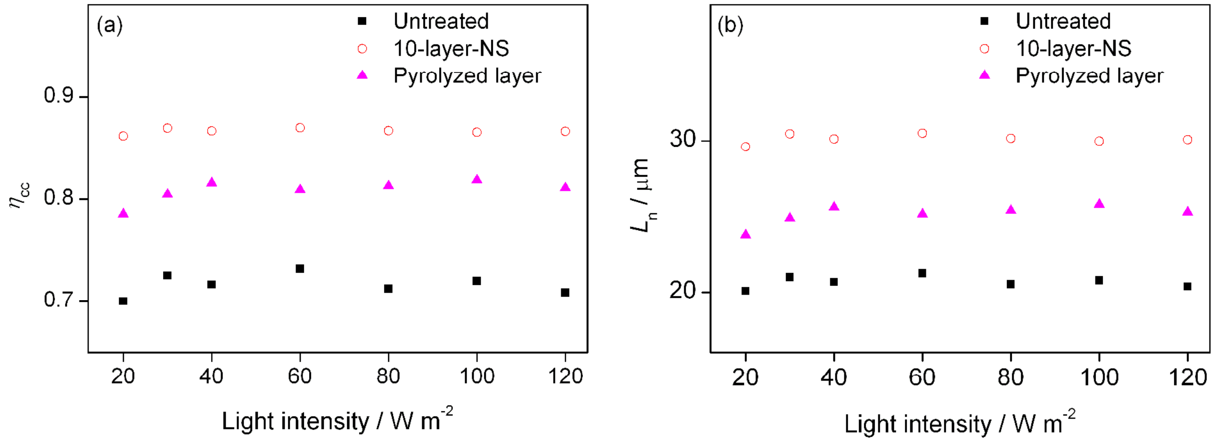

Figure 8. (a) Charge collection efficiency and (b) electron diffusion length as a function of light intensity

Effect on Photovoltage. The V_{oc} is dependent on the CB edge level and the accumulated charge density that relies on the photocurrent and charge recombination rate. As the untreated photoanode and the titania nanosheets pre-coated photoanode have comparable CB edge, their different V_{oc} should arise from their different charge densities at open circuit. The increase in charge density at the same light intensity from the untreated (90 μC cm^{-2}) to titania nanosheets pre-coated photoanode (146 μC cm^{-2}) causes voltage gain of 104 mV according to the relationship between V_{oc} and Q (Figure 5). The contribution to V_{oc} from increased Q is close to the observed enhancement of V_{oc}, implying that the photovoltage improvement is attributed to the retarded charge recombination caused by the pre-coated nanosheets layer. This can be understood as the complete coverage of FTO with titania nanosheets blocking collected electrons from recombination with the electrolyte. When the layer number is less than 10, the surface of FTO is partially covered, and hence the suppression of charge recombination is less efficient, resulting in slight increase in V_{oc}. However, for the layer number more than 10, the V_{oc} decreases with layer number despite the full coverage of FTO. This is ascribed to the decreased photocurrent.

Although the $TiCl_4$ treatment is also able to retard charge recombianiton,[24] it has negligible effect on the photovoltage according to the reported data[24] and our results (Figure 4), because the downward shift of CB edge caused by $TiCl_4$ treatment offsets the contribution to voltage from suppressed charge recombination.[24] From the viewpoint of photovoltage enhancement, pre-coating FTO with titania nanosheets is superior to the well-known $TiCl_4$ treatment[24] and the reported TiO_2 blocking layers[11-14,27] as well, where smaller photovoltage enhancements were obtained.

Effect on Photocurrent. Photocurrent relies upon light harvesting efficiency (LHE), electron injection efficiency and charge collection efficiency (η_{cc}). It is noted that the ultrathin titania nanosheet layer does not influence the LHE of the dye-loaded photoanode as the absorbance of dye-loaded 10-layer titania nanosheets is negligible as compared to that of the dye-loaded TiO_2 film. In the case of titania film with the same thickness adsorbing the same dye, the LHE should be same for the two photoanodes. As the CB edge does not shift upon pre-coating of titania nanosheets, the change of electron injection efficiency should be excluded. Thus, the photocurrent improvement is attributed to the enhanced charge collection efficiency (Figure 8). The presence of titania nanosheets improves the contact between FTO and TiO_2 film and hence increases charge collection efficiency.[11] In addition, covering the FTO surface with flat titania nanosheets can hinder the triiodides from recombination with collected electrons at the FTO surface, which is also favorable for getting high charge collection efficiency. Increasing the thickness of the blocking layer above 50 nm leads to decreased photocurrent. Particularly, when 200 nm titania nanosheet layer is pre-coated on FTO, the J_{sc} and *PCE* are even much lower than those of the untreated photoanode. This implies that thick titania nanosheets layer generates a barrier that obstructs electrons collected by the underlying FTO. For this reason, there is an optimal thickness of nanosheet blocking layer for best solar cell performance.

Conclusions

This work has demonstrated self-assembled titania nanosheet film as a unique blocking layer to improve the photovoltaic performance of DSSCs. The blocking effect depends on the layer thickness, and the optimal layer thickness is determined to be 50 nm for the best solar cell performance. This novel blocking layer increases J_{sc} by 45%, V_{oc} by 16% and *PCE* by 61%, as compared to the untreated cell. As a result, pre-coating of titania nanosheets onto FTO achieves power conversion efficiency of 10.48% with open-circuit photovoltage around 800 mV. The nanosheet blocking layer is superior to the reported TiO_2 nanoparticle blocking layers in enhancing efficiency. The advantage of nanosheet over nanoparticle is its flatness, which is possible to fully cover the conductive substrate with more and better contacts. Furthermore, the employed self-assembly technique provides excellent control of layer thickness, which is critical to get best blocking effect. Finally, the single crystal nature of flat nanosheet is favorable for fast electron transfer from photoanode to the substrate for efficient electron collection.[28,29] These results suggest that the titania nanosheet blocking layer would be an ideal approach to optimizing solar cell performance.

Acknowledgment

This work was financially supported by the National Basic Research Program (No. 2011CB933302) of China, STCSM (12JC1401500), Singapore-Berkeley Energy Research Institute (R279-000-393-592) and the Institute of Materials Research and Engineering core fund.

References

[1] Department of Chemistry, Lab of Advanced materials, iChEM (Collaborative Innovation Center of Chemistry for Energy Materials), Fudan University, 2205 Songhu Road, Shanghai 200438, P. R. China

[2] Department of Chemical and Biomolecular Engineering, National University of Singapore, Singapore 117576, Singapore

[3] Institute of Materials Research Engineering (A*STAR), 3 Research Link, Singapore 117602, Singapore

[*] Corresponding author. E-mail: zs.wang@fudan.edu.cn

§ Electronic Supplementary Information (ESI) available: See DOI: 10.1039/b000000x/

1. B. O'Regan and M. Grätzel, *Nature*, 1991, **353,** 737.
2. M. K. Nazeeruddin, A. Kay, I. Rodicio, R. Humphry-Baker, E. Müller, P. Liska, N. Vlachopoulos and M. Grätzel, *J. Am. Chem. Soc.*, 1993, **115,** 6382.
3. A. Yella, H.-W. Lee, H. N. Tsao, C. Yi, A. K. Chandiran, M. Nazeeruddin, E. W.-G. Diau, C.-Y. Yeh, S. M. Zakeeruddin and M. Grätzel, *Science*, 2012, **334,** 629.
4. M. Wang, N. Chamberland, L. Breau, J.-E. Moser, R.-H. Baker, B. Marsan, S. M. Zakeeruddin and M. Grätzel, *Nat. Chem.*, 2010, **2,** 385.
5. L. Kavan, J.-H. Yum, and M. Grätzel, *Nano Lett.*, 2011, **11,** 5501.
6. F. Gong, H. Wang, X. Xu, G. Zhou and Z.-S. Wang, *J. Am. Chem. Soc.*, 2012, **134,** 10953.
7. D. Wu, F. Zhu, J. Li, H. Dong, Q. Li, K. Jiang, D. Xu, *J. Mater. Chem.*, 2012, **22**, 11665.
8. D. Wu, X. Shi, H. Dong, F. Zhu, K. Jiang, D. Xu, *J. Mater. Chem. A*, 2014, **2**, 16276.
9. F. Fabregat-Santiago, J. Bisquert, G. Garcia-Belmonte, G. Boschloo and A. Hagfeldt, *Sol. Energy Mater. Sol. Cells*, 2005, **87,** 117.
10. P. J. Cameron and L. M. Peter, *J. Phys. Chem. B*, 2003, **107,** 14394.
11. M. S. Góes, E. Joanni, E. C. Muniz, R. Savu, T. R. Habeck, P. R. Bueno and F. Fabregat-Santiago, *J. Phys. Chem. C.*, 2012, **116,** 12415.
12. B. Yoo, K.-J. Kim, S.-Y. Bang, M. J. Ko, K. Kim and N.-G. Park, *J. Electroanal. Chem.*, 2010, **638,** 161.
13. S. Ito, P. Liska, P. Comte, R. Charvet, P. Pechy, U. Bach, L. Schmidt-Mende, S. M. Zakeeruddin, A. Kay, M. K. Nazeeruddin and M. Grätzel, *Chem. Commun.*, 2005, **34,** 4351.
14. J. Xia, N. Masaki, K. Jiang and S. Yanagida, *J. Phys. Chem. B*, 2006, **110**, 25222.
15. L. Kavan, N. Tétreault, T. Moehl and M. Grätzel, *J. Phys. Chem. C,* 2014, **118**, 16408.
16. M. H. Abdullah, M. J. N. Hart, D. Menzies, Y. Cheng, G. P. Simon and L. Spiccia, *C.R. Chimie*, 2006, **9**, 622.
17. H. Wang, J. Li, F. Gong, G. Zhou and Z.-S. Wang, *J. Am. Chem. Soc.*, 2013, **135,** 12627.
18. X. G. Han, Q. Kuang, M. Jin, Z. Xie and L. Zheng, *J. Am. Chem. Soc.*, 2009, **131,** 3152.
19. Z.-S. Wang, T. Sasaki, L. Z. Wang and M. Watanabe, *Chem. Mater.*, 2003, **15,** 807.
20. G. Decher, *Science*, 1997, **277,** 1232.
21. Z.-S. Wang, H. Kawauchi, T. Kashima and H. Arakawa, *Coord. Chem. Rev.*, 2004, **248,** 1381.
22. T. Sasaki, Y. Ebina, T. Tanaka, M. Harada and M. Watanabe, *Chem. Mater.*, 2001, **13,** 4661.
23. C. J. Barbé, F. Arendse, P. Comte, M. Jirousek, F. Lenzmann, V. Shklover and M. Grätzel, *J. Am. Ceram. Soc.*, 1997, **80,** 3157.
24. B. O'Regan, J. Durrant, P. Sommeling and N. Bakker, *J. Phys. Chem. C*, 2007, **111,** 14001.
25. G. Schlichthörl, S. Y. Huang, J. Sprague and A. J. Frank, *J. Phys. Chem. B*, 1997, **101,** 8141.
26. J. van de Lagemaat, N.-G. Park and A. J. Frank, *J. Phys. Chem. B*, 2000, **104,** 2044.
27. A. Alberti, G. Pellegrino, G. G. Condorelli, C. B. S. Morita, A. L. Magna and T. Miyasaka, *J. Phys. Chem. C* 2014, **118**, 6576.
28. Q. Huang, G. Zhou, L. Fang, L. Hu, Z.-S. Wang, *Energy Environ. Sci.* 2011, **4**, 2145.
29. Y. Cui, L. Zhang, K. Lv, G. Zhou, Z.-S. Wang, *J. Mater. Chem. A* 2015, **3**, 4477.

Table of Contents Entry

Self-Assembled Ultrathin Titania Nanosheets as Blocking Layers for Significantly Enhanced Photocurrent and Photovoltage of Dye-Sensitized Solar Cells

Lu Zhang,[1] Hong Sun,[1] Zhaosheng Xue,[2] Bin Liu,[2,3] Zhong-Sheng Wang[1,] *

[1] Department of Chemistry, Lab of Advanced materials, iChEM (Collaborative Innovation Center of Chemistry for Energy Materials), Fudan University, 2205 Songhu Road, Shanghai 200438, P. R. China
[2] Department of Chemical and Biomolecular Engineering, National University of Singapore, Singapore 117576, Singapore
[3] Institute of Materials Research Engineering (A*STAR), 3 Research Link, Singapore 117602, Singapore

* Corresponding author, E-mail: zs.wang@fudan.edu.cn, Tel/Fax: +86-21-51630345